QSAR, Pharmacophore and Molecular Docking Studies for the Design of Novel Arylamide-derived Inhibitors of *Mycobacterium tuberculosis*

Adama Niaré [a], Abadê Ange-Boris N'guessan [b], Akassa Marius Bernard Djako [a], Georges Stéphane Dembélé [c*], Mamadou Guy-Richard Koné [c] and Yaya Yéo [d]

[a] *Laboratoire de Physique Fondamentale et Appliquée (LPFA), University of Nangui Abrogoua, Abidjan 02, Côte d'Ivoire.*
[b] *Laboratoire d'Instrumentation, Image et Spectroscopie (L2IS), National Polytechnic Institute Felix Houphouët-Boigny (INPHB), Yamoussoukro, Côte d'Ivoire.*
[c] *Laboratory of Thermodynamics and Physico-chemistry of the Environment, UFR SFA, Nangui University 02 BP 801 Abidjan 02, Côte-d'Ivoire.*
[d] *Département de Sciences et Technologie, University Alassane Ouattara, Bouaké 1801, Côte d'Ivoire.*

Authors' contributions

This work was carried out in collaboration among all authors. All authors read and approved the final manuscript.

Original Research Article

_____

*Corresponding author: E-mail: 1997sageme@gmail.com;

ABSTRACT

Tuberculosis is an infectious disease caused by the bacterium *Mycobacterium tuberculosis*. It remains a significant public health challenge worldwide. In 2022, approximately 10.6 million people were diagnosed with tuberculosis, and 1.3 million individuals lost their lives to the disease. This manuscript presents our research focused on designing new inhibitors for the enoyl acyl carrier protein reductase (*InhA*) of *Mycobacterium tuberculosis*. This enzyme is vital as it plays a key role in the type II fatty acid biosynthesis pathway of *M. tuberculosis*. To conduct our study, we utilized computer simulations, specifically docking and quantitative structure-activity relationship (QSAR) analysis on free molecules. We applied these methods to a series of arylamide-derived inhibitors, the efficacy of which was proposed by He et al. The results obtained from our docking and QSAR analyses confirm the robustness of the molecules identified by He et al., based on their experimental activities. Furthermore, the docking results facilitated the generation of a pharmacophore model, which was instrumental in designing a new inhibitor of *Mycobacterium tuberculosis InhA*. This new compound demonstrates enhanced activity compared to previously identified inhibitors. Such advancements could significantly contribute to the development of novel treatments for *tuberculosis* and help address this critical global health issue.

Keywords: QSAR model; pharmacophore model; molecular docking; molecular modeling; Mycobacterium tuberculosis; InhA.

1. INTRODUCTION

Humanity, in its perpetual development, has long been confronted with serious epidemic problems, such as tuberculosis, which has been around for millennia. Efforts to combat it have been an integral part of human history. Although tuberculosis has never caused the greatest panic among populations of all epidemics, it has nevertheless been one of the most deadly through the centuries. Tuberculosis (TB) is a contagious, endemo-epidemic disease of essentially human-to-human transmission, caused by the *Mycobacterium tuberculosis* (M.T.) complex [1]. It is one of the leading causes of death from infectious diseases worldwide, particularly in low- and middle-income countries [2]. TB is still a worldwide scourge. Pulmonary involvement is the most frequent localization and the usual source of transmission. However, from 1920 onwards, with the advent of effective chemotherapy, the introduction of preventive measures such as the Bilié de Calmette et Guérin (BCG) vaccine in 1921, and the discovery of numerous effective antibiotics such as rifampicin from 1944 to 1965, the decline in tuberculosis was real [1,3,4]. The incidence of tuberculosis fell steadily by 5% a year from 1953 to 1985, and eradication seemed possible [4]. As early as 1986, there was a resurgence of TB worldwide, following an increase in the number of cases initially reported, and the role of HIV/AIDS infection in this resurgence appeared very likely [1]. Despite current progress, tuberculosis remains a major public health problem, with incidence, prevalence and mortality still high. This calls for a multi-sectoral approach, the integration of health into all policies, and a paradigm shift from TB control to the elimination of the epidemic. Furthermore, the elimination of the tuberculosis epidemic is underpinned by decisive factors including strong government leadership, universal access to treatment, access to all vulnerable populations, collaboration with civil society and communities, and the adoption of new technologies [5]. Faced with the emergence of multi-resistant or ultra-resistant strains, it is urgent to enrich the therapeutic arsenal by developing new drugs capable of simplifying and reducing the duration of current treatment. This is one of the reasons that motivated us to carry out this work, which is part of the design of new inhibitors of enoyl acyl carrier protein reductase (*InhA*). The general aim of our work is to propose new, more active and more effective molecules capable of inhibiting *InhA*, one of the main enzymes involved in the *M. tuberculosis* type II fatty acid biosynthesis pathway, by means of molecular docking, QSAR of molecules confirmed by a pharmacophore model, and virtual screening of the arylamide using Computer Simulated Molecular Modeling.

2. MATERIALS AND METHODS

2.1 Ligands (Arylamide Derivatives)

The molecules used are arylamide derivatives. They have therapeutic properties that can inhibit the action of *InhA*. Their common part is shown Fig. 1.

The entire series was obtained by substitutions at two ring positions as shown (Fig. 2). Their experimental inhibitory concentrations IC50exp [5,6] cover a sufficiently wide concentration range to serve well for the construction of a reliable QSAR model of InhA inhibition.

2.2 Molecular Docking

Binding energy is the energy of attachment of a ligand (L) to a receptor (R). Its value in this work is approximated to that of the free enthalpy of formation of the enzyme-inhibitor complex. These binding energies ($\Delta Gbinding$) were calculated for each complex after their minimization using the "Calculate Binding Energy" protocol.

Chemical equilibrium of the ligand-receptor interaction

$$L + R \rightleftharpoons C \tag{1}$$

$$\Delta G_{complex} = G_{complex} - G_{ligand} - G_{receptor} \tag{2}$$

$$\Delta \Delta G_{(receptor+ligand)} = \Delta G_{(receptor+ligand)} - \Delta G_{(receptor+endogenous\ ligand)} \tag{3}$$

$$\Delta \Delta G_{binding} = \Delta G_{binding} - \Delta G_{binding\ ref} \tag{4}$$

$\Delta G_{binding\ ref}$ is the binding energy of the most active ligand.

As the IC_{50}^{exp} of the various inhibitors are known from the literature, the pIC_{50}^{exp} is calculated using the following formula:

$$pIC_{50}^{exp} = -\log_{10}\left(IC_{50}/10^6\right) \tag{5}$$

2.3 QSAR of Free Molecules

The principle of QSAR methods is to implement a mathematical relationship linking molecular properties called descriptors and biological activity for a series of similar chemical compounds using data analysis methods. To this end, we have freely optimized the training set molecules on the STO-3G base with Gaussian version 03 [7]. After optimization, the following descriptors were extracted from the log file (output file): exact polarizability $(\alpha_{xx}\ \alpha_{yy}\ \alpha_{zz})$, dipole moment, Hartree-Fock energy (E_{hf}), HOMO energies (E_{HO}) and LUMO (E_{BV}). Based on the descriptors identified, other descriptors were calculated, namely mean polarizability (α_e), anisotropy γ^2, chemical potential (μ), electronegativity (χ), ionization potential (PI), electron affinity (AE), η: chemical hardness, σ :overall softness and ω electrophilicity index using the following formulas [8]:
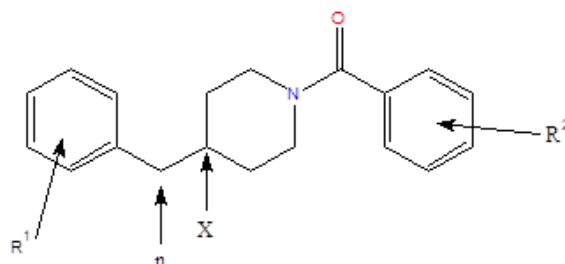
$$AE = -E_{BV} \tag{6}$$

$$PI = -E_{HO} \tag{7}$$

$$\eta = \frac{1}{\sigma} = PI - AE \tag{8}$$

$$\mu = -\frac{AE + PI}{2} = -\chi \tag{9}$$

$$\omega = \frac{\mu^2}{2\eta} = \frac{\chi^2}{2\eta} \tag{10}$$

$$\alpha_e = \frac{1}{3}\left(\alpha_{xx} + \alpha_{yy} + \alpha_{zz}\right) \tag{11}$$

$$\gamma^2 = \frac{1}{2}((\alpha_{xx} - \alpha_{yy})^2 + (\alpha_{yy} - \alpha_{zz})^2 + (\alpha_{zz} - \alpha_{xx})^2 \tag{12}$$

Where:
n: number of carbon chains
X: number of nitrogen atoms (0 or 1)

Fig. 1. Skeleton of arylamide derivatives

41-1-14 (IC50= 0.12 μM)

44-9 (IC50= 1.04 μM)

32-5 (IC50= 1.85 μM)

33-7 (IC50=9.47 μM)

31-7 (IC50= 0.99 μM)

47-2 (IC50= 0.39 μM)

22-4 (IC50= 1.35 μM)

23-2 (IC50= 10.66 μM)

37-8 (IC50=7.74 μM)

21-1 (IC50=3.07 μM)

34-10 (IC50= 6.73 μM)

27-2 ($IC50 = 16.64 \mu M$)

28-1-18 (IC50= 6.26μM)

43-2 (IC50=0.91 μM)

29-1 (IC50= 3.07 μM)

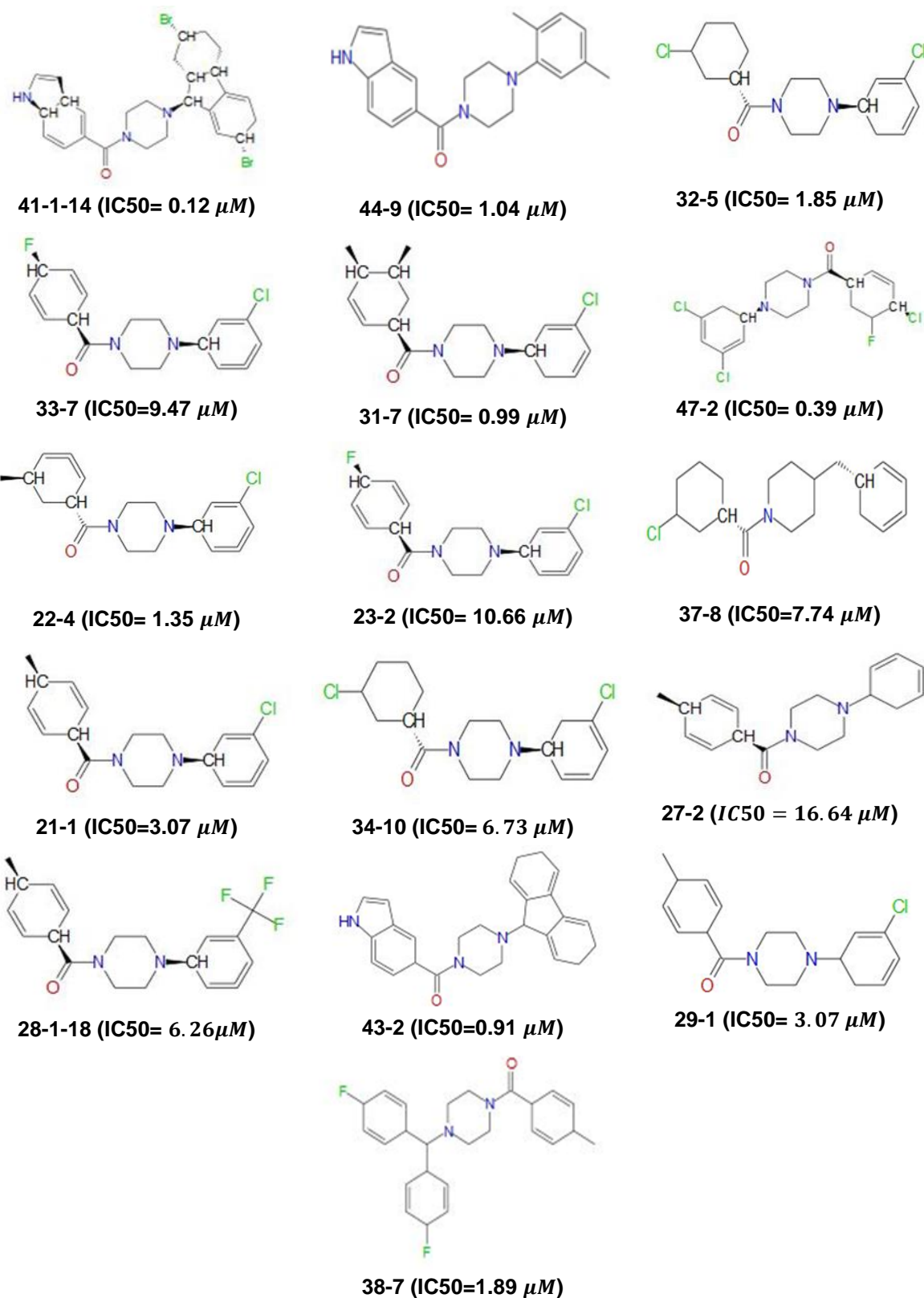**38-7 (IC50=1.89 μM)**

Fig. 2. Ligands in test and validation sets

2.4 The Pharmacophore Model

A pharmacophore is a set of active centers that a molecule must have to be functional. Each of these active centers is assigned 3D coordinates, a volume (generally spherical) and physicochemical properties (lipophilicity, hydrogen bond donor/acceptor, etc.). This model can be used to describe how a molecule binds to the active site of a protein. The design of new analogues based on the pharmacophore model generated. The new "test set" of poses retained after calculation of the binding energy will be used to generate the pharmacophore. The pharmacophore activity model proposed here will help explain the variation in activity of different ligands.
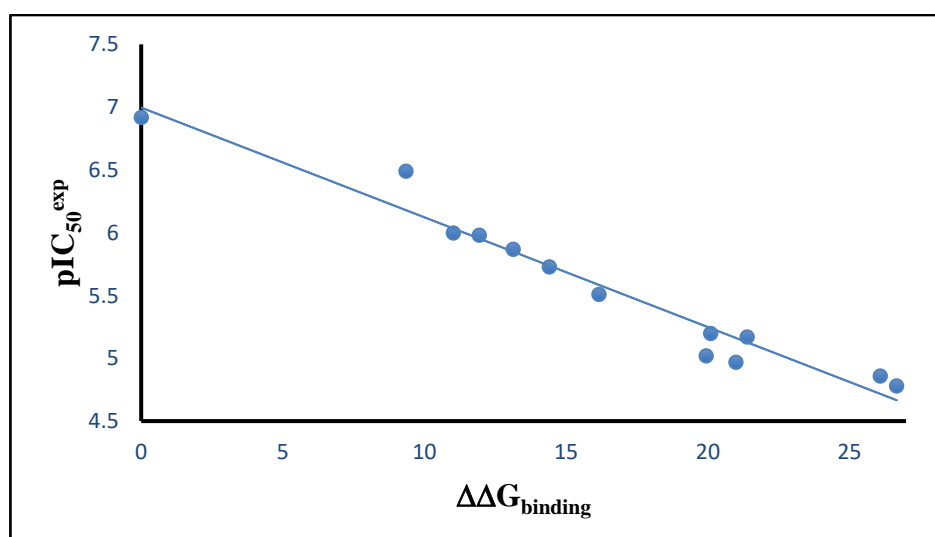
3. RESULTS AND DISCUSSION

3.1 Molecular Docking

Molecular docking of 16 endogenous ligand-derived inhibitors from the 2NSD active site. Calculation of binding energies ($\Delta G_{binding}$) gave us the results assigned in Table 1.

The correlation curve between the variation in binding energies and the experimental pIC50s of the 13 inhibitors in the test set is shown in Fig. 3.

Table 1. Protein-ligand binding energy and biological activities

| Nature	LIGANDS	$\Delta G_{binding}$ (kcal/mol)	$\Delta\Delta G_{binding}$ (kcal/mol)	IC_{50}^{exp} (μM)	pIC_{50}^{exp}
Molecules more active	41-1-14	-53.15	0	0.12	6.92
	47-2-10	-43.79	9.35	0.39	6.49
	31-7	-42.13	11.02	0.99	6
	44-9	-41.22	11.93	1.04	5.98
Medium-active molecules Active	22-4	-40.02	13.13	1.35	5.87
	32-8	-38.74	14.41	1.85	5.73
	21-2	-36.99	16.16	3.07	5.51
	28-1-18	-33.05	20.10	6.26	5.20
	34-10	-31.76	21.39	6.73	5.17
Molecules Weakly active	33-7	-33.20	19.95	9.47	5.02
	23-2	-32.16	20.99	10.66	4.97
	26-20	-27.06	26.09	13.87	4.86
	27-2	-26.48	26.67	16.64	4.78

Fig. 3. Plot illustrating the correlation between pIC_{50}^{exp} and the $\Delta\Delta G_{binding}$ energy component.

Table 2. Statistical data and linear regression

Number of compounds n	**13**
Correlation coefficient of the regression line R^2	0.96
Cross-validation coefficients R^2_{CV}	0.96
Standard error of the regression (σ)	0.55
Fisher test (F)	283.57
Risk of error	5%
Experimental biological activity range (μM)	$0.12 - 16.64$

Table 3. Comparison of experimental and theoretical biological activity values in the validation set
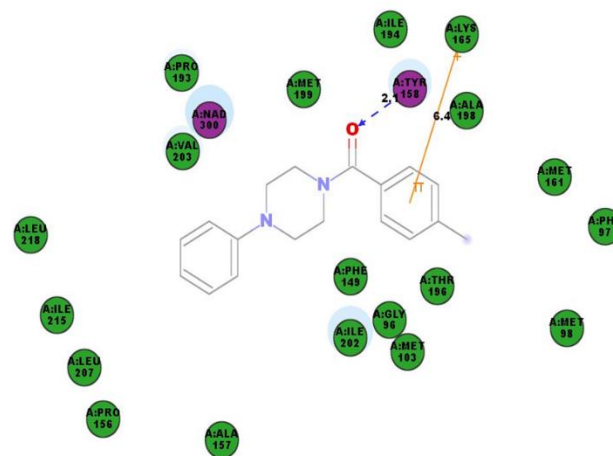
Ligands	$\Delta G_{binding}$ (kcal/mol)	$\Delta\Delta G_{binding}$ (kcal/mol)	IC_{50}^{exp} (μM)	pIC_{50}^{exp}	pIC_{50}^{pred}	$pIC_{50}^{Pred} / pIC_{50}^{exp}$
43-2	-36.33	16.82	0.91	6.04	5.52	0.91
38-7	-48.59	4.55	1.89	5.72	6.58	1.15
29-1	-33.52	19.63	3.07	5.51	5.28	0.96
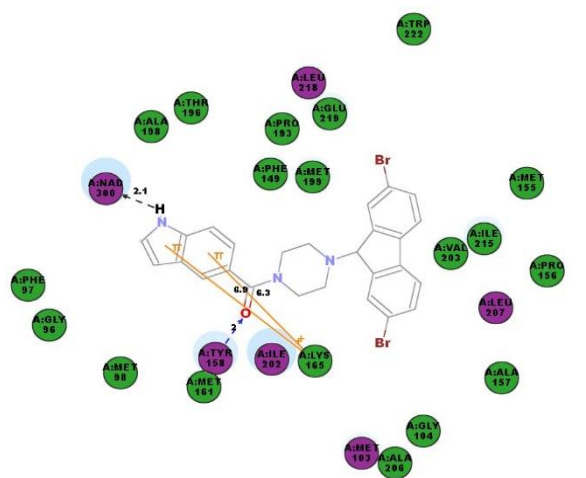
Fig. 4. 2D diagram of the active ligand 41-1-14
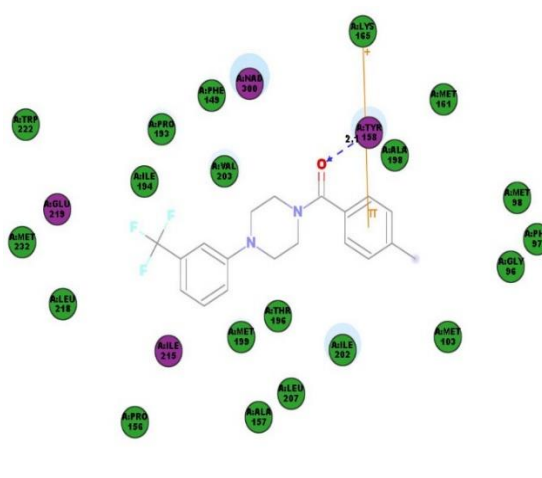
Fig. 5. 2D diagram of the moderately active ligand 28-1-18

Fig. 6. 2D diagram of the less active ligand 27-2

The results in Table 2 show, relatively high values of the regression coefficient and Fischer test of the correlation involving ΔΔGbinding. All these values indicate, that there is a strong relationship between the binding model and the experimental model of the arylamide series. The theoretical activities of the "validation set" inhibitors are obtained from the following equation :

$$pIC_{50}^{pred} = -0.0951 * \Delta\Delta G_{binding} + 6.9611 \quad (13)$$

For the molecules in the validation set, theoretical activities will be compared with experimental activities in order to judge this prediction. The prediction is good if the ratio $pIC_{50}^{pred}/pIC_{50}^{exp}$ is close to 1.

The various reports $pIC_{50}^{pred}/pIC_{50}^{exp}$ in Table 3 are close to 1. The results of these reports show that the docking model is reliable and that the activities of new analogues can be estimated from it. This interaction ensures the ligand's rigidity, and these interactions help to enhance a molecule's activity.

In all these complexes, hydrogen bond and π-bond interactions are observed.There are two π-bond interactions that are established between the ligands and the site LYS165 in complex 41-1-14 and one in the other complexes (28-1-18 and 27-2). The hydrogen bond interaction established between the ligand and TYR158 is observed in all complexes and another hydrogen bond between the cofactor and ligand in complex 41-1-

14. The particularity of the most active ligand is that it establishes more interactions with the amino acids of the active site, giving it greater activity. These interactions ensure the ligand's rigidity and stability, making it better than the medium- and less-active ligands, which establish fewer π-bonds and hydrogen bonds. The π-bond established between the ligands and the LYS165 site in complex 28-1-18 occurs at a distance of 2.1 Å, in contrast to complex 27-2 where the bond is established at a distance of 2.6 Å. This explains why the ligand in complex 28-1-18 has good activity compared with the ligand in complex 27-2, and why a molecule is all the more stable when the bonds are made at a short distance.

Hydrogen bonds are important for protein folding, conformational changes and protein/ligand recognition. On the ligand side, they affect the physico-chemical properties of molecules, such as solubility and membrane permeability, which are crucial elements in drug development.

3.2 QSAR of Molecules

Molecular descriptor values calculated using Excel software [9] are listed in Table 4.

100 models were obtained, of which GFATempModel_67 was selected as it takes into account some interesting physico-chemical descriptors, namely: Apol, LUMO or BV energy and dipole moment.

From these values (Table 5), we obtained the following curve:

Table 4. Values of calculated molecular descriptors

Ligands	E_HUMO (ua)	E_LUMO (ua)	Dipole moment (Debye)	$\gamma^2(\text{Å}^6)$	$\alpha_e(\text{Å}^3)$	$P^2(D^2)$
41-1-14	-0.22	0.24	4.70	5232.09	176.51	22.13
47-2-10	-0.25	0.20	2.29	7334.59	127.38	5.25
31-7	-0.23	0.24	4.62	6806.32	127.19	21.33
44-9	-0.21305	0.24	2.34	8954.21	139.47	5.47
22-4	-0.23	0.24	4.22	6917.28	121.85	17.81
32-8	-0.23	0.22	3.20	6043.29	119.39	10.18
21-2	-0.23	0.24	4.29	7846.59	150.28	18.38
28-1-18	-0.22	0.24	2.78	2481.73	124.09	7.71
34-10	-0.25	0.22	3.19	6044.12	119.39	10.17
33-7	-0.23	0.23	3.10	6853.37	116.33	9.64
23-2	-0.23	0.23	3.10	6853.39	116.33	9.64
26-20	-0.23	0.23	3.41	1078.66	113.99	11.67
27-2	-0.21	0.24	1.81	3240.75	114.37	3.28

Table 5. GFA model 67 and pIC_{50}^{exp} values for the 13 ligands in the test set

Ligands	GFA MODEL 67	pIC_{50}^{exp}
41-1-14	6.92	7.13
47-2-10	6.41	6.24
31-7	6	5.74
44-9	5.98	5.62
22-4	5.87	5.43
32-8	5.73	5.64
21-2	5.22	5.25
28-1-18	5.20	5.46
34-10	5.17	5.44
33-7	5.11	5.04
23-2	5.02	5.30
26-20	4.97	5.30
27-2	4.78	4.79
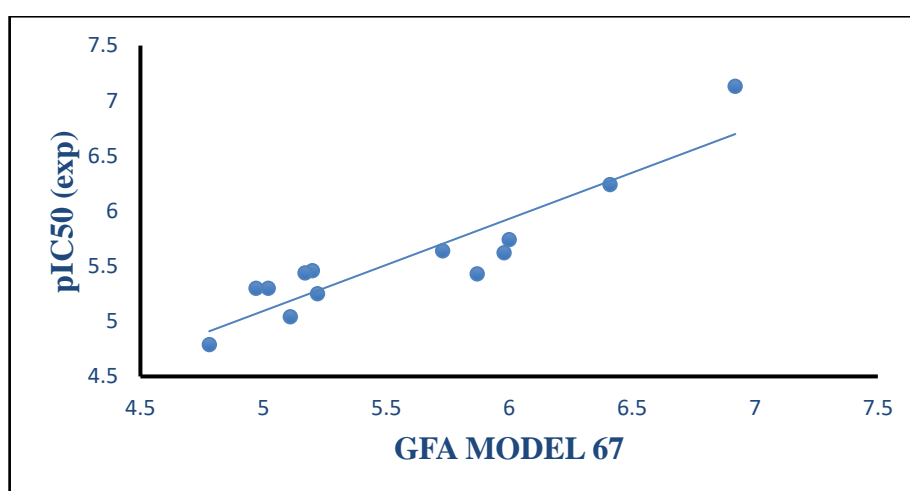
Fig. 7. Graph illustrating the correlation between pIC_{50}^{exp} and the GFA MODEL 67 component

Table 6. Statistical data and linear regression

Number of compounds n	**13**
Correlation coefficient of the regression line R^2	0.83
Cross-validation coefficients R_{CV}^2	0.82
Standard error of the regression (σ)	0.27
Fisher test (F)	55.69
Risk of error	5%
Experimental biological activity range (μM)	0.12 – 16.64

The equation of the correlation line is of the following form:

$$pIC_{50}^{pred} = -5.5684 + 0.0005701 * Apol + 15.497 * Ebv - 0.00086 * Mdip \qquad (14)$$

The values of the ratios $pIC_{50}^{exp}/pIC_{50}^{pred}$ of the ligands of the "validation set" being close to 1, these testify well to the predictive quality of the QSAR model selected.

3.3 Pharmacophore Model

The interaction generation protocol of Discovery Studio's molecular modeling program [10] provides the functionality of the protein's active

site pharmacophore. The Inha protein features a hydrophobic pocket within its active site. This hydrophobic pocket is very large and made up of long alkyl chains.

The 3D-RQSA pharmacophore for Inha inhibition was generated from the active conformations of the 13 ligands in the test set and evaluated by the 3 others in the validation set, covering a wide range of experimental activities (0.12-16.64 µM). estimated activities (IC_{50}^{est}) and experimental data are shown in Table 8.

Using on the one hand the estimated values of activities (IC_{50}^{est}) from Table 8 and the formula, we have calculated the estimated activities (pIC_{50}^{est}). Fig. 8 shows the correlation curve between experimental pIC50s and estimated pIC50s for the 13 inhibitors in the test set.

Table 7. Comparison between pIC_{50}^{pred} and pIC_{50}^{exp} of the ligands in the validation set

LIGANDS	IC_{50}^{exp}	pIC_{50}^{exp}	pIC_{50}^{pred}	Rapport
43-2	0.91	6.04	7.22	0.84
38-7	1.89	5.72	7.15	0.80
29-1.	3.07	5.51	5.6	0.98

Table 8. Experimental activity values and those predicted by the pharmacophore model

LIGANDS	IC_{50}^{est} (μM)	pIC_{50}^{est}	IC_{50}^{exp} (μM)	pIC_{50}^{exp}
41-1-14	0.088	7.06	0.12	6.92
44-9	0.86	6.06	1.04	5.98
22-8	1.61	5.79	1.35	5.86
31-7	1.67	5.78	0.99	6
47-2-10	1.73	5.76	0.39	6.41
32-8	2.36	5.63	1.85	5.73
34-10	3.16	5.50	6.73	5.17
28-1-18	3.44	5.46	6.26	5.20
27-2	4.46	5.35	16.64	4.78
21-2	4.75	5.32	3.07	5.51
26-20	4.85	5.31	13.87	4.86
23-2	4.97	5.30	10.66	4.97
33-7	5.40	5.27	9.47	5.02
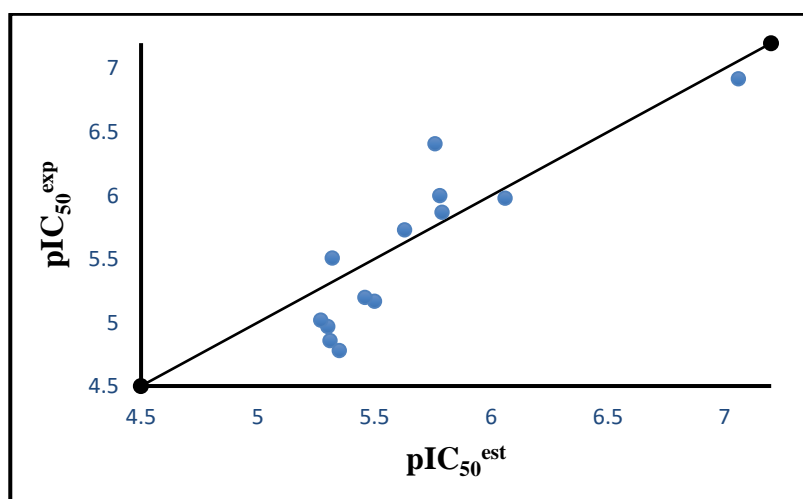
Fig. 8. Correlation graph of experimental inhibitory activity versus predicted inhibitory activity

**Table 9. Statistical data and linear regression**

Number of compounds n	**13**
Correlation coefficient of the regression line R^2	0.82
Cross-validation coefficients R_{CV}^2	0.80
Standard error of the regression (σ)	0.78
Fisher test (F)	50.72
Risk of error	5%
Experimental biological activity range (μM)	0.12 − 16.64

The equation of the correlation line is as follows:

$$pIC_{50}^{exp} = 0.988 * pIC_{50}^{est} + 0.0669 \tag{15}$$

Table 10. Comparison between pIC_{50}^{est} and pIC_{50}^{exp} of the ligands in the validation set

LIGANDS	IC_{50}^{est}	pIC_{50}^{est}	pIC_{50}^{exp}	Rapport
43-2	0.37	6.43	6.04	1.06
38-7	25.04	4.60	5.72	0.81
29-1	27.21	4.56	5.51	0.83
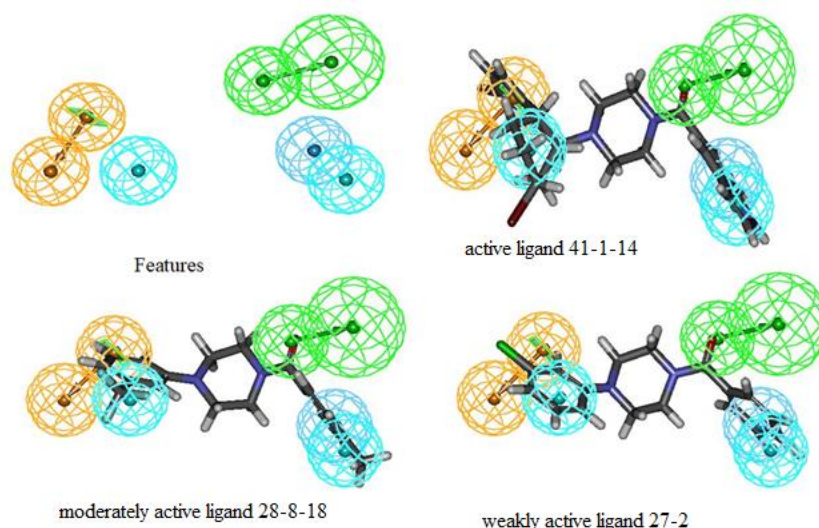
Fig. 9 Features et ligands épousant les features

Ratio values $pIC_{50}^{est}/pIC_{50}^{exp}$ of the ligands in the "validation set" are close to 1, indicating a good predictive quality of our pharmacophore model. The model is therefore reliable and can be used to predict the biological activities of new InhA-inhibiting arylamide acid analogues. The selected model (Fig. 10) is composed of four (04) features: one (01) hydrogen bond acceptor "HBA" in green, one (01) aromatic ring "Aromatic" in orange, one (01) aromatic ring "Hydrophobic Aromatic" in light blue and one (01) aromatic ring "Hydrophobic Aliphatic" in light blue. The arrow represents the projection for acceptor and donor features.

Based on our model with good predictive inhibitory power, we proceeded to design a new analog (7-8-1) more active than those proposed by He et al. The strategy adopted consists in taking into account the perceptible presence of hydrophobic functionalities included in the pharmacophore model coupled with hydrogen bond donor and acceptor substitutions.

3.4 Screening the Virtual Library

This part of the work consists in creating a library from the skeleton of a molecule. To do this, we used the skeleton of the most active molecule

(41-1-14) in the "test set", on which the substitutions were made in order to propose more active molecules. After calculating the molecular properties, this library is filtered using the LIPINSKI [11].

We created a virtual library of 900 molecules. When we applied the LIPINSKI rules to filter the virtual library for orally-administerable molecules, we obtained a virtual library of 878 molecules. This was then screened using PH4. After

screening, we selected molecule (7-8-1) from among those proposed by PH4.

From each QSAR model developed in this work we have expressed the predicted activity of the molecule (7-8-1). Fig. 11 shows the selected molecule and Fig. 10 the alignment of this molecule in the pharmacophore model.

The tables (Table 10, Table 11, Table 12) show the activity of the molecule selected in each model.
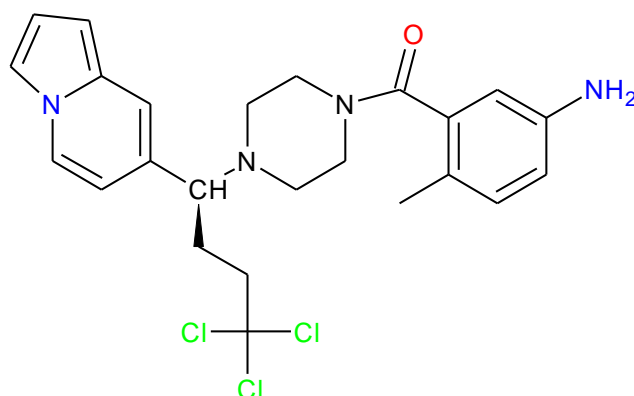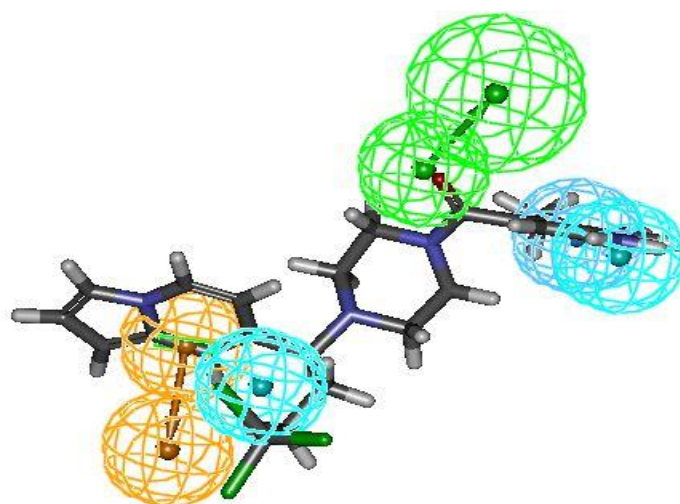

Fig. 10. Analog structure (7-8-1)

Fig. 11. Alignment of the molecule (7-8-1) in the PH4 model

Table 11. Value of $pIC_{50}^{théo}$ from the QSAR model docking of the selected molecule

LIGAND	$\Delta G_{binding}$(kcal/mol)	$\Delta\Delta G_{binding}$(kcal/mol)	$pIC_{50}^{théo}$
7-8-1	-61.99	-8.84	7.74

Equation 13 was used to calculate the $pIC_{50}^{théo}$ of the (7-8-1) molecule.

Table 12. Value of $pIC_{50}^{théo}$ from the QSAR model of the selected molecule

LIGAND	Apol	E_{bv}(kcal/mol)	$M_{dipolaire}$ (D)	$pIC_{50}^{théo}$
7-8-1	16505.90	0.13	3.53	8.30

Equation 14 was used to calculate the $pIC_{50}^{théo}$ of the molecule (7-8-1).

Table 13. pIC50est value based on the PH4 model for the selected molecule

LIGAND	IC_{50}^{est} (μM)	pIC_{50}^{est}
7-8-1	0.01	7.96

From equation 15 we determined the pIC_{50}^{est} of the molecule (7-8-1).

4. CONCLUSION

The aim of this work is to identify new molecules derived from arylamides with good inhibitory activity to combat tuberculosis. The specific objective of this work is very important, given the emergence of strains that are multi-resistant or ultra-resistant to available antibiotics, and the large number of tuberculosis cases worldwide highlighting the urgent need for effective, well-tolerated treatment for these particular forms of tuberculosis. Hence the interest in researching new molecules capable of acting on these strains. The different methods used, namely molecular docking, free QSAR of molecules and the pharmacophore model, have enabled us to establish the correlation between biological activity and a set of real numbers called descriptors, to predict the mode of ligand binding and the free energies of formation of the different complexes. The pharmacophore model built from the best poses retained after molecular docking enabled us to observe the regions of the active site likely to be occupied by proton-donor groups, hydrophobic groups and aromatic rings of inhibitors of InhA, one of the main enzymes involved in the type II fatty acid biosynthesis pathway of *M. tuberculosis*. Based on this information, we were able to predict the activity of a potential new analog which is more active than the ligand in our training set.

DISCLAIMER (ARTIFICIAL INTELLIGENCE)

Author(s) hereby declare that NO generative AI technologies such as Large Language Models (ChatGPT, COPILOT, etc.) and text-to-image generators have been used during the writing or editing of this manuscript.

COMPETING INTERESTS

Authors have declared that no competing interests exist.

REFERENCES

1. Aubry P, Gaüzère B-A. Centre rené labusquière. Institute of Tropical Medicine. Bordeaux (France). 2018;33076.
2. Lienhardt C. Tuberculosis in the world today: Issues, research and perspectives. Presses De Sciences; 2011.
3. Souidi L. The prevalence of pulmonary tuberculosis in Oujda-Anggad. Mohammed V University. Rabat; 2014.
4. GIRON J, et al. Imaging of thoracic tuberculosis approaching the year 2000. Encycl. Med. Surg. Radiodiagnostics – Heart – Lung. 1998,1:232-390;A-10:19.
5. World Health Organization Regional Office for Africa. Framework for the implementation of the "WHO End TB Strategy" in the African Region during the period 2016–2020; 2017.
6. He X, Alian A, Ortiz de Montellano PR. Inhibition of the *Mycobacterium tuberculosis* enoyl acyl carrier protein reductase InhA by arylamides. Bioorganic & Medicinal Chemistry. 2007;15(121): 6649–6658.
7. Frisch MJ, Trucks GW, Schlegel HB, Scuseria GE, Robb MA, Cheeseman JR, Montgomery JA, Jr. Vreven T, Kudin KN, Burant JC, Millam JM, Iyengar SS, Tomasi J, Barone V, Mennucci B, Cossi M, Gaussian 03 G, Revision C02, Gaussian, Inc., Wallingford CT, 2004.
8. Koopmans T. Über die zuordnung von wellenfunktionen und

eigenwerten zu den einzelnen elektronen eines atoms. Physica. 1934;1–6: 104–113.

9. Microsoft Corporation. Microsoft excel; 2018.
Avaliable:https://office.microsoft.com/excel.

10. Accelrys Software Inc. Discovery studio modeling environment. San Diego, CA; 2009.

11. Lipinski CA. Lead- and drug-like compounds: The rule-of-five revolution. Drug Discov Today Technol. 2004;1(14): 337-41

Peer-review history:
The peer review history for this paper can be accessed here:
https://www.sdiarticle5.com/review-history/128051